

Modeling chiral criticality*

BENGT FRIMAN

GSI Helmholtzzentrum für Schwerionenforschung, D-64291 Darmstadt, Germany

AND

GÁBOR ANDRÁS ALMÁSI

GSI Helmholtzzentrum für Schwerionenforschung, D-64291 Darmstadt, Germany

AND

KRZYSZTOF REDLICH

ExtreMe Matter Institute EMMI, GSI, D-64291 Darmstadt, Germany

University of Wrocław, Institute of Theoretical Physics, PL 50-204 Wrocław,
Poland

We discuss the critical properties of net-baryon-number fluctuations at the chiral restoration transition in matter at non-zero temperature and net-baryon density. The chiral dynamics of quantum chromodynamics (QCD) is modeled by the Polykov-loop extended Quark-Meson Lagrangian, that includes the coupling of quarks to temporal gauge fields. The Functional Renormalization Group is employed to account for the criticality at the phase boundary. We focus on the ratios of the net-baryon-number cumulants, χ_B^n , for $1 \leq n \leq 4$. The results are confronted with recent experimental data on fluctuations of the net-proton number in nucleus-nucleus collisions.

PACS numbers: PACS numbers come here

1. Introduction

Lattice QCD (LQCD) results imply that at vanishing and small values of baryon chemical potential, μ_B , strongly interacting matter undergoes a smooth crossover transition from the hadronic phase to the quark-gluon

* Presented at CPOD 2016 in Wrocław

plasma, where the spontaneously broken chiral symmetry is restored [1, 2]. The order of the transition in the limit of massless u and d quarks is a subtle issue, and still under debate [3]. Here we assume that the transition in this limit is second order, belonging to the $O(4)$ universality class. Owing to the sign problem, the nature of the transition at higher net-baryon densities is not settled by first principle LQCD studies. However, in effective models of QCD, it is found that, at sufficiently large μ_B , the systems can exhibit a first order chiral phase transition. The endpoint of this conjectured transition line in the (T, μ_B) - plane, is the chiral *critical point* (CP) [4, 5]. At the CP, the system exhibits a 2^{nd} order phase transition, which belongs to the $Z(2)$ universality class [6].

Due to the restriction of present LQCD calculations to small net-baryon densities, effective models that belong to the same universality class as QCD, e.g., the Polyakov-loop extended, Nambu-Jona-Lasinio (PNJL) [7–9] and Quark-Meson (PQM) models [10–15], have been employed to study the chiral phase transition for a broad range of thermal parameters.

One of the strategic goals of current experimental and theoretical studies of chiral symmetry restoration in QCD is to unravel the phase diagram of strongly interacting matter and to clarify whether a chiral CP exists. A dedicated research program at RHIC, the beam energy scan, has been established to explore these issues in collisions of heavy ions at relativistic energies [16]. By varying the beam energy at RHIC, the properties of strongly interacting matter in a broad range of net-baryon densities, corresponding to a wide range in baryon chemical potential, $20 \text{ MeV} < \mu_B < 500 \text{ MeV}$ [17, 18], can be studied. To study the phase structure, the fluctuations of conserved charges have been proposed as probes [19–23]. These are experimentally accessible and reflect the criticality of the chiral transition.

First data on net-proton-number fluctuations, which are used as a proxy for fluctuations of the net-baryon number, have been obtained in heavy-ion collisions by the STAR Collaboration at RHIC energies [24–26]. The STAR data on the variance, skewness and kurtosis of net proton number, are intriguing and have stimulated a lively discussion on their physics origin and interpretation [27].

In the following, we focus on the properties and systematics of the cumulants of net-baryon-number fluctuations near the chiral phase boundary. Our studies are performed in the Polyakov-loop extended Quark-Meson model which includes coupling of quarks to temporal gauge fields. To account for the $O(4)$ and $Z(2)$ critical fluctuations near the phase boundary, we employ the Functional Renormalization Group [28–30]. We present results for ratios of cumulants obtained on the phase boundary and on a freezeout line determined by fitting the skewness ratio, following [31, 32]. These are confronted with the corresponding experimental values of the

STAR collaboration.

2. The Polyakov–quark–meson model

The PQM model is a low energy effective approximation to QCD formulated in terms of the light quark $q = (u, d)$ as well as scalar and the pseudoscalar meson $\phi = (\sigma, \vec{\pi})$ fields. The quarks are coupled to the background Euclidean gluon field A_μ , with vanishing spatial components, which is linked to the Polyakov loop

$$\Phi = \frac{1}{N_c} \left\langle \text{Tr}_c \mathcal{P} \exp \left(i \int_0^\beta d\tau A_0 \right) \right\rangle. \quad (1)$$

The resulting Lagrangian of the model reads

$$\begin{aligned} \mathcal{L} = & \bar{q} (i\gamma^\mu D_\mu - g(\sigma + i\gamma_5 \vec{\tau} \vec{\pi})) q + \frac{1}{2} (\partial_\mu \sigma)^2 + \frac{1}{2} (\partial_\mu \vec{\pi})^2 \\ & - U_m(\sigma, \vec{\pi}) - \mathcal{U}(\Phi, \bar{\Phi}; T) - \frac{1}{2} m_\omega^2 \omega^2, \end{aligned} \quad (2)$$

where $D_\mu = \partial_\mu - iA_\mu$. The parameters of the mesonic potential

$$U_m(\sigma, \vec{\pi}) = \frac{\lambda}{4} (\sigma^2 + \vec{\pi}^2)^2 + \frac{m^2}{2} (\sigma^2 + \vec{\pi}^2) - H\sigma, \quad (3)$$

are tuned to vacuum properties of the σ and $\vec{\pi}$ mesons. We use the Polyakov-loop potential $\mathcal{U}(\Phi, \bar{\Phi}; T)$ determined in [33].

We compute the thermodynamics of this model, including fluctuations of the scalar and pseudoscalar meson fields within the framework of the FRG method. The Polyakov loop is treated on the mean-field level. Its value is tuned such that a stationary point of the thermodynamic potential is reached at the end of the RG calculation.

In the FRG framework, the effective average action Γ_k , which interpolates between the classical and the full quantum action, is obtained by solving the renormalization group flow equation [28]

$$\partial_k \Gamma_k[\phi] = \frac{1}{2} \text{Tr} \left[\left(\Gamma_k^{(2)}[\phi] + R_k \right)^{-1} \partial_k R_k \right], \quad (4)$$

where ϕ denotes the quantum fields considered, Tr is a trace over the fields, over momentum and over all internal indices. The regulator function R_k suppresses fluctuations at momenta below k . Thus, effects of fluctuations of quantum fields are included shell by shell in momentum space, starting from a UV cutoff scale Λ . We employ the optimized regulator introduced by Litim [34]. Details of the calculation can be found in [32].

3. Net-baryon-number cumulants and the phase boundary

The chiral Lagrangian introduced above shares the chiral critical properties with QCD. In particular, at moderate values of the chemical potential, the PQM model exhibits a chiral transition belonging to the $O(4)$ universality class. For larger values of μ , it reveals a $Z(2)$ critical endpoint, followed by a first order phase transition [6]. Consequently, the PQM model embodies the generic phase structure expected for QCD, with the universal $O(4)$ and $Z(2)$ criticality encoded in the scaling functions. Furthermore, due to the coupling of the quarks to the background gluon fields, the PQM model incorporates "statistical confinement", i.e., the suppression of quark and diquark degrees of freedom in the low temperature, chirally broken phase [7]. Consequently, by studying fluctuations of conserved charges in the PQM model, one can explore the influence of chiral symmetry restoration and of "statistical confinement" on the cumulants in different sections of the chiral phase boundary. The baryon- and quark-number cumulants of order n , χ_B^n and χ_q^n , and the baryon-number cumulant ratios, $\chi_B^{n,m}$, are defined as

$$\chi_B^n = \frac{\chi_q^n}{3^n} = \frac{1}{3^n T^{4-n}} \frac{\partial^n \Omega(T, \mu_q)}{\partial \mu_q^n}, \quad \chi_B^{n,m} = \frac{\chi_B^n(T, \mu_B)}{\chi_B^m(T, \mu_B)}. \quad (5)$$

In the following we focus on ratios of net-baryon-number susceptibilities that can be related to experimentally measurable quantities:

$$\chi_B^{1,2}(T, \mu_B) = M/\sigma^2, \quad \chi_B^{3,1}(T, \mu_B) = S_B \sigma^3/M, \quad \chi_B^{4,2}(T, \mu_B) = \kappa \sigma^2 \quad (6)$$

where M is the mean, σ the variance, S_B the skewness and κ the kurtosis of the net-baryon-number distribution.

At vanishing chemical potential, all odd susceptibilities of the net baryon number vanish, owing to the baryon-antibaryon symmetry. In addition, in the $O(4)$ universality class, the second and fourth order cumulants remain finite at the phase transition temperature at $\mu_q = 0$ in the chiral limit, implying that only sixth and higher order susceptibilities diverge. Thus, for physical quark masses, only higher order cumulants, χ_B^n with $n > 4$, can exhibit $O(4)$ criticality at $\mu_q = 0$ [23]. A further consequence of the baryon-antibaryon symmetry is the equality of the ratios

$$\chi_B^{2m-1, 2n-1} = \chi_B^{2m, 2n} \quad (7)$$

for any integer m and $n \geq 1$ at $\mu_q = 0$. For $\chi_B^{3,1}$ and $\chi_B^{4,2}$, the equality at small μ_q can also be seen by comparing the right panel of Fig. 1 to the left panel of Fig. 2.

At finite net-baryon density the singularity at the $O(4)$ critical line is stronger than at $\mu_q = 0$. Thus, in this case the third-order cumulant and all

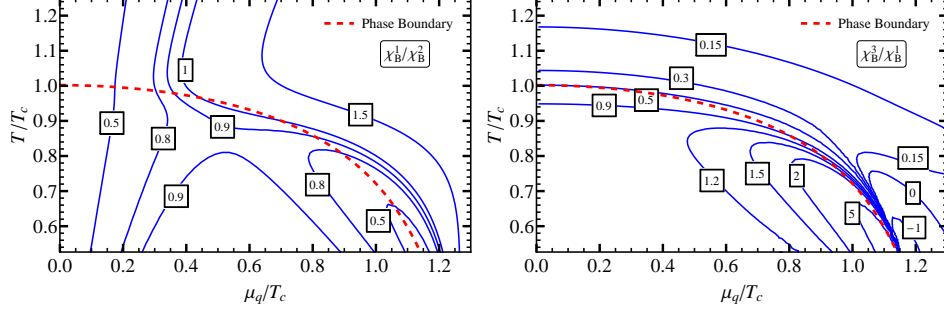


Fig. 1. Contour plots of the ratios χ_B^1/χ_B^2 and χ_B^3/χ_B^1 in the (T, μ_q) -plane, computed in the PQM model. The broken lines indicate the location of the chiral crossover phase boundary.

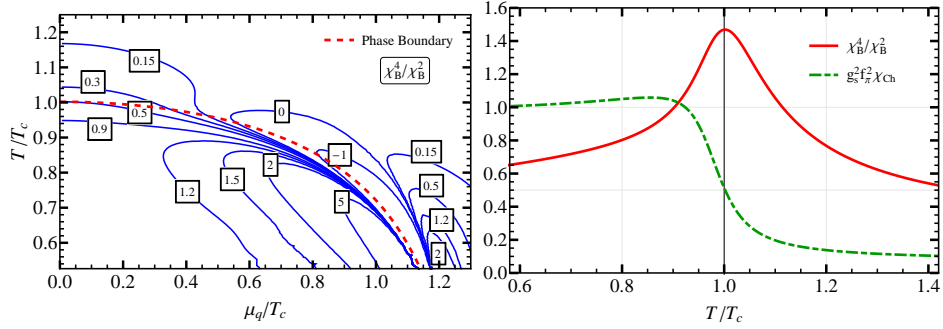


Fig. 2. Left: contour plot of the kurtosis ratio, χ_B^4/χ_B^2 , in the (T, μ_q) plane. Right: temperature dependence of ratios of net-baryon-number cumulants, $\chi_B^3/\chi_B^1 = \chi_B^4/\chi_B^2$ in the PQM model at $\mu_q = 0$.

higher-order ones diverge at the $O(4)$ line. The second order cumulant χ_B^2 remains finite, and diverges at the tricritical point and for non-zero quark masses, at the CP.

In Fig. 1 we show contour plots of the ratios $\chi_B^{1,2}$ and $\chi_B^{3,1}$ in the (T, μ_q) plane. As noted above, all odd cumulants vanish at $\mu_q = 0$. Consequently, $\chi_B^{1,2}|_{\mu_q=0} = 0$ for any T , while the ratio $\chi_B^{3,1}|_{\mu_q=0}$ is non-vanishing. As indicated in Fig. 1, the ratio $\chi_B^{3,1}$ decreases with temperature, and depends weakly on the chemical potential. Thus, the ratio $\chi_B^{3,1}$ can be used as a measure of the temperature.

In Fig. 2 we show contour plots of the ratios $\chi_B^{4,2}$ and results on the temperature dependence of the ratio $\chi_B^{3,1} = \chi_B^{4,2}$ of net-baryon-number susceptibilities at $\mu_q = 0$, together with the variance of the chiral condensate,

χ_{ch} . The location of the maximum of the chiral susceptibility, χ_{ch} , defines the pseudo-critical temperature, T_c .

At small μ_q/T , the properties of the first four susceptibilities, χ_B^n with $n = 1, \dots, 4$, and consequently their ratios, near the chiral crossover are dominantly affected by the coupling of the quarks to the Polyakov loop, and the resulting statistical confinement. The critical chiral dynamics, i.e. the $O(4)$ and $Z(2)$ criticality at the chiral crossover transition and at the CP, respectively, unfolds at larger μ/T . Near the CP, there is a strong variation of the cumulants with T and μ_q , which increases with the order of cumulants.

4. Net-baryon cumulant ratios and freeze-out in heavy ion collisions

In heavy-ion collisions, the thermal fireball formed in the quark-gluon plasma phase undergoes expansion and passes through the QCD phase boundary at some point (μ_q, T) , which depends on the collision energy, \sqrt{s} . Analysis of ratios of particle multiplicities indicate that at high beam energies (small values of μ_q/T), the freeze out occurs at or just below the phase boundary. Thus, the beam energy dependence of net-baryon-number susceptibilities can provide insight into the structure of the QCD phase diagram and information on the existence and location of the CP. Consequently, it is of phenomenological interest to compute the properties of fluctuations of conserved charges along the chiral phase boundary. Since there, the critical structure and the relations between different susceptibilities are by and large governed by the universal scaling functions, the generic behavior of ratios of net-baryon-number susceptibilities can be explored also in model calculations.

A comparison of results obtained in the PQM model with data, requires a correspondence between the collision energy \sqrt{s} and the thermal parameters (μ_q, T) . Here we employ the phenomenological relation, obtained by analysing the freeze-out conditions in terms of the hadron-resonance-gas model (HRG) [17, 18]. We then use the resulting dependence of μ_B and T on \sqrt{s} to assign a value for the ratio μ_q/T to each of the STAR beam energies. We note that, for $\mu_q/T < 1$, the phenomenological freeze-out line coincides within errors with the crossover phase boundary obtained in lattice QCD [2, 36]. This motivates a comparison of model results on net-baryon-number fluctuations near the phase boundary with data. A similar analysis was first done using LQCD results in Ref. [31].

In Fig. 3, we show the STAR data on net-proton-number susceptibility ratios and the corresponding PQM model results on net-baryon-number fluctuations computed along the phase boundary. The model results for the

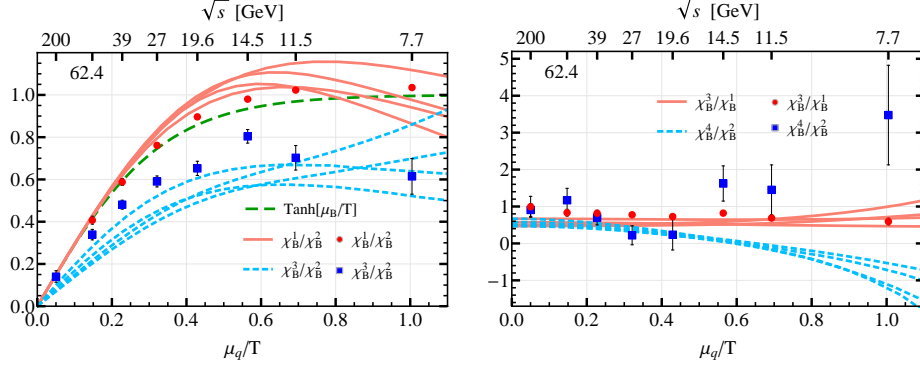


Fig. 3. Ratios of cumulants of net-baryon-number fluctuations in the PQM model, computed along the chiral phase boundary, for four sets of model parameters [32]. Also shown are the preliminary STAR data [25, 26], assuming the relation between the ratio (μ_q/T) and the collision energy obtained by analysing the chemical freeze-out conditions [18, 35, 36]. The green dashed line in the left figure shows the baseline result for $\chi_B^{1,2}$, $\tanh(3\mu_q/T)$.

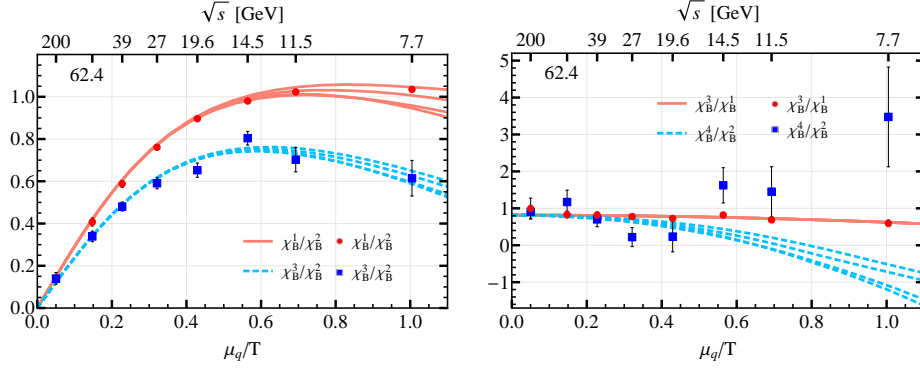


Fig. 4. Ratios of cumulants of net-baryon-number fluctuations in the PQM model along the freezeout line, obtained by fitting χ_B^3/χ_B^1 to the STAR data. The four sets of model parameters used and the preliminary STAR data shown, are the same as in Fig. 3.

ratios $\chi_B^{1,2}$, $\chi_B^{3,1}$ and $\chi_B^{3,2}$ are in qualitative agreement with the data in the whole energy range. For the kurtosis ratio, $\chi_B^{4,2}$, this is the case also up to the SPS energy, i.e., for $\sqrt{s} \geq 20$ GeV. However, for $\mu_q/T > 0.5$, the data on the kurtosis ratio exhibits a qualitatively different dependence on μ_q/T than expected for the critical behavior of $\chi_B^{4,2}$, as the CEP is approached along the phase boundary.

In the comparison of model predictions with data in Fig. 3, we as-

sume, that the freezeout of the net-baryon-number fluctuations tracks the chiral phase boundary. Clearly, this assumption provides a qualitative understanding of the data. In order to obtain a more quantitative description, we follow Refs. [31, 37, 38], and determine the freezeout conditions by fitting the data on the $\chi_B^{3,1}$ ratio, using the \sqrt{s} -dependence of μ_q/T obtained from the fit of the HRG model to particle multiplicities [18, 35, 36].

In Fig. 4 we show the fluctuation ratios along the freezeout line that is fixed through the skewness data. The model results are obtained for four sets of initial conditions introduced in [32]. Fig. 4 clearly shows that, along the freezeout line, the spread of all fluctuations ratios considered for the various parameter sets is much weaker than that observed in Fig. 3 along the phase boundary. This indicates that moderate changes of the sigma mass and modifications of the form of the Polyakov loop potential may lead to a shift in the temperature scale but essentially no change of the relative structure of the cumulant ratios.

The results presented in Fig. 4 clearly show that the model provides a very good description of the data on $\chi_B^{1,2}$ and $\chi_B^{3,2}$. Also the kurtosis data, obtained at higher collision energies, are consistent with model results. However, at $\sqrt{s} < 20$ GeV the latter again exhibits a different trend, with the data increasing rapidly at lower energies, while the model result keeps decreasing.

The comparison of model results on ratios of net-baryon-number susceptibilities with the STAR data in Figs. 3 and 4 shows that the data, with the exception of kurtosis at low energies, follow general trends expected due to critical chiral dynamics and general considerations. We note that the ratios of net-baryon-number susceptibilities near the phase boundary involving net-baryon-number cumulants χ_B^n with $n \geq 3$ are controlled mainly by the scaling functions in the $O(4)$ and $Z(2)$ universality classes, respectively. This observation indicates, that by measuring fluctuations of conserved charges in heavy-ion collisions, we are indeed probing the QCD phase boundary, and thus accumulating evidence for chiral symmetry restoration.

However, as discussed above, there are several uncertainties and assumptions which must be thoroughly understood before the QCD phase boundary can be pinned down with confidence. Possible contributions to fluctuation observables from effects not related to critical phenomena, like e.g. baryon-number conservation [39] and volume fluctuations [40, 41] are being explored. We mention in particular the rather strong sensitivity of higher order net-proton-number cumulants on the transverse momentum range imposed in the analysis of the STAR data. Nevertheless, it is intriguing that the dynamics of this model provides a good description of the STAR data (except for χ_B^4 at the lowest energies), without all these effects of non-critical origin. It remains an important task to assess the effect of

theses additional sources of fluctuations in the whole energy range probed by the experiments.

Acknowledgments

We acknowledge stimulating discussions with Peter Braun-Munzinger, Frithjof Karsch and Nu Xu. The work of B.F. and K.R. was partly supported by the Extreme Matter Institute EMMI. K. R. also acknowledges partial supports of the Polish National Science Center (NCN) under Maestro grant DEC-2013/10/A/ST2/00106. G. A. acknowledges the support of the Hessian LOEWE initiative through the Helmholtz International Center for FAIR (HIC for FAIR).

REFERENCES

- [1] Y. Aoki, G. Endrodi, Z. Fodor, S. D. Katz, and K. K. Szabo, [Nature](#) **443**, 675 (2006).
- [2] S. Borsanyi, Z. Fodor, C. Hoelbling, S. D. Katz, S. Krieg, C. Ratti, and K. K. Szabo (Wuppertal-Budapest), [JHEP](#) **09**, 073 (2010).
- [3] C. Bonati, P. de Forcrand, M. D’Elia, O. Philipsen, and F. Sanfilippo, [Phys. Rev. D](#) **90**, 074030 (2014).
- [4] M. Asakawa and K. Yazaki, [Nucl. Phys. A](#) **504**, 668 (1989).
- [5] A. M. Halasz, A. D. Jackson, R. E. Shrock, M. A. Stephanov, and J. J. M. Verbaarschot, [Phys. Rev. D](#) **58**, 096007 (1998).
- [6] B.-J. Schaefer and J. Wambach, [Phys. Rev. D](#) **75**, 085015 (2007).
- [7] K. Fukushima, [Physics Letters B](#) **591**, 277 (2004).
- [8] C. Ratti, M. A. Thaler, and W. Weise, [Phys. Rev. D](#) **73**, 014019 (2006).
- [9] C. Sasaki, B. Friman, and K. Redlich, [Phys. Rev. D](#) **75**, 074013 (2007).
- [10] B.-J. Schaefer, J. M. Pawłowski, and J. Wambach, [Phys. Rev. D](#) **76**, 074023 (2007).
- [11] B.-J. Schaefer, M. Wagner, and J. Wambach, [Phys. Rev. D](#) **81**, 074013 (2010).
- [12] T. K. Herbst, J. M. Pawłowski, and B.-J. Schaefer, [Phys. Lett. B](#) **696**, 58 (2011).
- [13] V. Skokov, B. Stokic, B. Friman, and K. Redlich, [Phys. Rev. C](#) **82**, 015206 (2010).
- [14] V. Skokov, B. Friman, E. Nakano, K. Redlich, and B. J. Schaefer, [Phys. Rev. D](#) **82**, 034029 (2010).
- [15] V. Skokov, B. Friman, and K. Redlich, [Phys. Rev. C](#) **83**, 054904 (2011).
- [16] M. M. Aggarwal *et al.* (STAR), (2010), [arXiv:1007.2613 \[nucl-ex\]](#).
- [17] P. Braun-Munzinger, K. Redlich, and J. Stachel, [arXiv:nucl-th/0304013 \[nucl-th\]](#).

- [18] J. Cleymans, H. Oeschler, K. Redlich, and S. Wheaton, *Phys. Rev. C* **73**, 034905 (2006).
- [19] M. A. Stephanov, K. Rajagopal, and E. V. Shuryak, *Phys. Rev. Lett.* **81**, 4816 (1998).
- [20] M. A. Stephanov, K. Rajagopal, and E. V. Shuryak, *Phys. Rev. D* **60**, 114028 (1999).
- [21] M. Asakawa, U. W. Heinz, and B. Muller, *Phys. Rev. Lett.* **85**, 2072 (2000).
- [22] S. Jeon and V. Koch, *Phys. Rev. Lett.* **85**, 2076 (2000).
- [23] B. Friman, F. Karsch, K. Redlich, and V. Skokov, *The European Physical Journal C* **71**, 1694 (2011).
- [24] L. Adamczyk *et al.* (STAR Collaboration), *Phys. Rev. Lett.* **112**, 032302 (2014).
- [25] X. Luo (STAR), *PoS CPOD2014*, 019 (2015).
- [26] X. Luo, *Nuclear Physics A* **956**, 75 (2016).
- [27] Y. Akiba, S. Esumi, K. Fukushima, H. Hamagaki, T. Hatsuda, T. Hirano, and K. Shigaki, *Nucl. Phys. A* **956**, pp.1 (2016).
- [28] C. Wetterich, *Phys. Lett. B* **301**, 90 (1993).
- [29] T. R. Morris, *Int. J. Mod. Phys. A* **09**, 2411 (1994).
- [30] J. Berges, N. Tetradis, and C. Wetterich, *Phys. Rept.* **363**, 223 (2002).
- [31] A. Bazavov *et al.*, *Phys. Rev. Lett.* **109**, 192302 (2012).
- [32] G. Almasi, B. Friman, and K. Redlich, (2017), [arXiv:1703.05947 \[hep-ph\]](#).
- [33] P. M. Lo, B. Friman, O. Kaczmarek, K. Redlich, and C. Sasaki, *Phys. Rev. D* **88**, 074502 (2013).
- [34] D. F. Litim, *Phys. Rev. D* **64**, 105007 (2001).
- [35] A. Andronic, P. Braun-Munzinger, and J. Stachel, *Nucl. Phys. A* **772**, 167 (2006).
- [36] A. Andronic, P. Braun-Munzinger, and J. Stachel, *Phys. Lett. B* **673**, 142 (2009).
- [37] G. A. Almási, B. Friman, and K. Redlich, *Nuclear Physics A* **956**, 356 (2016).
- [38] W.-j. Fu and J. M. Pawłowski, *Phys. Rev. D* **93**, 091501 (2016).
- [39] A. Bzdak, V. Koch, and V. Skokov, *Phys. Rev. C* **87**, 014901 (2013).
- [40] V. Skokov, B. Friman, and K. Redlich, *Phys. Rev. C* **88**, 034911 (2013).
- [41] P. Braun-Munzinger, A. Rustamov, and J. Stachel, *Nuclear Physics A* **960**, 114 (2017).